Spin dynamics in the pseudogap state of a high-temperature superconductor

V. HINKOV[1], P. BOURGES[2], S. PAILHÈS[2], Y. SIDIS[2], A. IVANOV[3], C. D. FROST[4], T. G. PERRING[4], C. T. LIN[1], D. P. CHEN[1] AND B. KEIMER[1]*

[1]Max Planck Institute for Solid State Research, D-70569 Stuttgart, Germany
[2]Laboratoire Léon Brillouin, CEA-CNRS, CE-Saclay, 91191 Gif-sur-Yvette, France
[3]Institut Laue-Langevin, 156X, 38042 Grenoble cedex 9, France
[4]ISIS Facility, Rutherford Appleton Laboratory, Chilton, Didcot OX11 0QX, UK
*e-mail: b.keimer@fkf.mpg.de

Published online: 16 September 2007; doi:10.1038/nphys720

The pseudogap is one of the most pervasive phenomena of high-temperature superconductors[1]. It is attributed either to incoherent Cooper pairing setting in above the superconducting transition temperature, T_c, or to a hidden order parameter competing with superconductivity. Here, we use inelastic neutron scattering from underdoped $YBa_2Cu_3O_{6.6}$ to show that the dispersion relations of spin excitations in the superconducting and pseudogap states are qualitatively different. Specifically, the extensively studied 'hour glass' shape of the magnetic dispersions in the superconducting state[2–4] is no longer discernible in the pseudogap state and we observe an unusual 'vertical' dispersion with pronounced in-plane anisotropy. The differences between superconducting and pseudogap states are thus more profound than generally believed, suggesting a competition between these two states. Whereas the high-energy excitations are common to both states and obey the symmetry of the copper oxide square lattice, the low-energy excitations in the pseudogap state may be indicative of collective fluctuations towards a state with broken orientational symmetry predicted in theoretical work[5–8].

The pseudogap manifests itself in various experimental probes as a depletion of spectral weight on cooling below a doping-dependent characteristic temperature, T^*. The origin of the pseudogap remains the focus of significant debate. For instance, recent experiments have provided evidence of vortex-like excitations below T^* akin to those in the superconducting state[9]. Other experiments[10] suggest the presence of a novel magnetic order breaking time-reversal symmetry, again setting in around T^*.

Inelastic neutron scattering directly probes the microscopic magnetic dynamics and can thus serve as a particularly incisive test of microscopic models of the cuprates. Recent work on non-superconducting $La_{2-x}(Sr,Ba)_xCuO_4$ and in the superconducting state of $YBa_2Cu_3O_{6+x}$ has uncovered tantalizing evidence of a 'universal' spin excitation spectrum independent of material-specific details[2–4,11,12]. The dispersion surface comprises upward- and downward-dispersing branches merging at the wavevector $\mathbf{Q}_{AF}$, which characterizes antiferromagnetic order in the undoped parent compounds. The spectrum thus resembles an 'hour glass' in energy–momentum space. Investigations of the superconducting state of twin-free $YBa_2Cu_3O_{6+x}$ (that is, single crystals with a unique orientation of the two in-plane axes a and b throughout the entire volume) have revealed a two-dimensional geometry of the lower branch, with a modest in-plane anisotropy of the spectral weight that increases with decreasing excitation energy[13]. The hour-glass spectrum and its in-plane anisotropy have stimulated theoretical work in the framework of both itinerant and local-moment pictures of the electron system[14–19].

Previous measurements of twinned $YBa_2Cu_3O_{6+x}$ samples seemed to indicate that the spin excitation spectrum in the pseudogap state is simply a broadened version of the spectrum in the superconducting state[20–22]. However, the detailed investigation of the geometry and dispersion of spin excitations in the pseudogap state reported here reveals that both spectra are distinctly different.

The measurements were carried out on an array of twin-free single crystals of underdoped $YBa_2Cu_3O_{6.6}$ with superconducting $T_c = 61$ K (see the Methods section). Figure 1 shows representative raw data in the superconducting state at 5 K, in the pseudogap state just above T_c, and at room temperature. The incommensurability, δ, and the spectral weight of the constant-energy cuts are generally different in the two in-plane directions in reciprocal space, H and K, and show a complex dependence on energy and temperature (see the Methods section for definitions). A synopsis of the entire data set is shown in Fig. 2 at two temperatures above and below T_c.

The main result here is the change of the topology of the dispersion surface from the superconducting to the pseudogap state. First, we focus on the spectrum in the superconducting state (Fig. 1, 5 K). Starting from low excitation energies, δ first decreases with increasing energy, so that the incommensurate peaks merge at $\mathbf{Q}_{AF}$ at an energy of $E_{res} = 37.5$ meV. For $E > E_{res}$, δ increases again, so that the spectrum forms the hour-glass dispersion (Fig. 2a,b) already familiar from previous work[2,4,11,23]. In the pseudogap state, however, the singularity at E_{res} is no longer discernible, and δ is only weakly energy dependent over a wide energy range including E_{res} (Fig. 2c,d and Supplementary Information). This constitutes a qualitative difference of the spectra in the superconducting and pseudogap states.

The spin excitations in both states also differ markedly with respect to their a–b anisotropy. In the superconducting state, constant-energy cuts of the magnetic spectral weight at energies below E_{res} form ellipses with aspect ratios of about 0.8

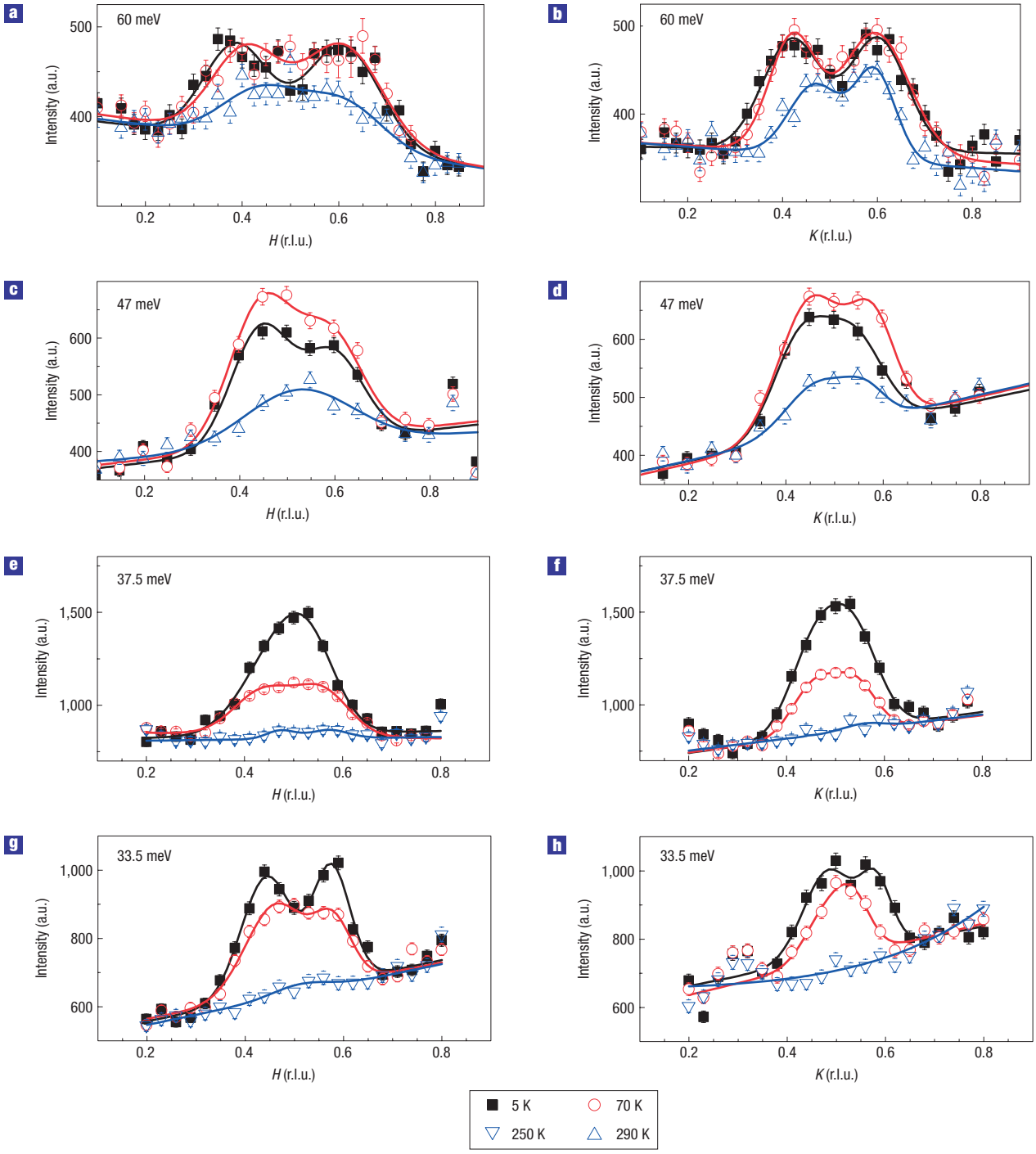

Figure 1 Energy evolution of the in-plane magnetic excitations around Q_{AF} for different temperatures. a–h, The energy transfer was fixed to 60 meV (**a**,**b**), 47 meV (**c**,**d**), 37.5 meV (**e**,**f**) and 33.5 meV (**g**,**h**). Panels **a**,**c**,**e** and **g** show scans along the *a* axis and panels **b**,**d**,**f** and **h** scans along the *b* axis. The lines are the results of fits to gaussian profiles. We show the raw triple-axis data; the only data processing applied is a subtraction of a constant at 250 and 290 K to account for the increased background from multiphonon scattering. Corrections for the Bose factor are small and were not applied to the data. The final wavevector was fixed to 2.66 Å^{-1} for $E \leq 37.5$ meV and to 4.5 Å^{-1} above. The error bars indicate the statistical error.

(Figs 1g,h and 3a). In the pseudogap state, the Q extent of the signal decreases significantly along b^* such that incommensurate peaks can hardly be resolved, Fig. 1h. In contrast, the flat-top profiles along a^* are well described by two broad peaks displaced from $\mathbf{Q}_{AF}$, Fig. 1g, and we can set an upper bound of 0.6 on the ratio of δ along b^* and a^*. The intensity distribution of the high-energy excitations, on the other hand, hardly changes between the superconducting and pseudogap states (Figs 1a,b and 3b). It is also much more

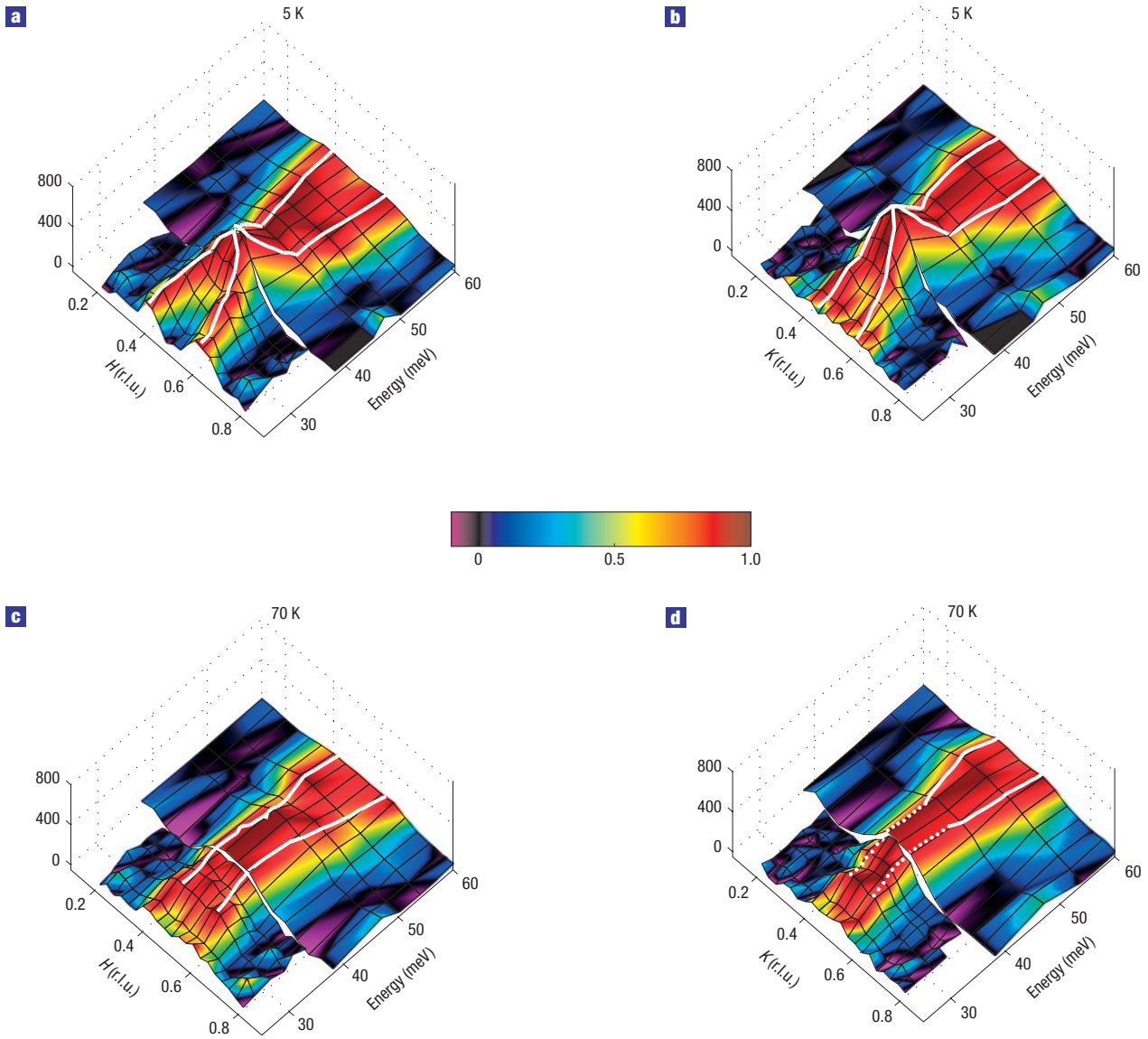

Figure 2 Colour representation of the magnetic intensity, obtained from triple-axis scans. a,**b**, The superconducting regime. **c**,**d**, The regime just above T_c. Scans along the *a* axis (H, -1.5, -1.7) (**a**,**c**) and the *b* axis (1.5, K, 1.7) (**b**,**d**). To obtain a meaningful colour representation, the intensity at 250 K was subtracted for $E < 38$ meV and the data were corrected for a **Q**-linear background at all energies. At each individual energy, the colour scale was normalized to the peak intensity of the scan, allowing a better comparison of the Q extent at different energies. The final wavevector was fixed to 2.66 Å^{-1} below 38 meV and to 4.5 Å^{-1} above. Scans taken at the overlapping energy 38 meV were used to bring both energy ranges to the same scale. The crossings of black lines represent measured data points. The white lines connect the fitted peak positions of the constant-energy cuts. The dotted lines represent upper bounds on the incommensurability.

isotropic than the low-energy profiles. Specifically, the ratio of δ along a^* and b^* is 0.95 ± 0.07 as obtained from an analysis of the time-of-flight (TOF) and triple-axis data. Moreover, there is no amplitude suppression along b^* and the anisotropy in the peak widths is also less pronounced than at low energies (0.16 ± 0.02 and 0.13 ± 0.02 r.l.u. along a^* and b^*, respectively).

On cooling below T_c, the spectral rearrangement associated with the formation of the downward-dispersing branch of the hour glass results in a sharp upturn of the intensity at points along this branch (Fig. 4a,b), whereas at $\mathbf{Q}_{AF}$ and 30 meV there is only a broad maximum at T_c (Fig. 4c). This is a further manifestation of the qualitative difference between the superconducting- and pseudogap-state spectra. In the pseudogap state, the spectral weight at energies at and below E_{res} declines uniformly with increasing temperature at all **Q** values and vanishes around $T^* \approx 200$ K. T^* is comparable to the temperature below which the pseudogap manifests itself in other experimental probes[1,9,10]. Corresponding constant-energy cuts show that for $T > T^*$, the low-energy spectral weight is severely depleted over the entire Brillouin zone below an energy $E^* \sim 40$ meV, Fig. 1e–h (see also Supplementary Information Notes and ref. 20). In contrast, at energies above E^* the spectral weight is only moderately reduced on heating above T^* (Fig. 1a,b). We can thus distinguish a third temperature regime above T^*, with a magnetic excitation spectrum differing distinctly from the spectra in the superconducting state and just above T_c.

Two aspects of our data in the pseudogap state merit further comment. First, we observe the low-energy magnetic spectral weight to increase on cooling below T^*, in contrast to the loss of spectral weight indicated by nuclear magnetic resonance (NMR) data[1]. However, it should be kept in mind that the energy scales probed by NMR and neutron scattering differ by three orders of magnitude. The behaviour we observe can be viewed as a pile-up of spectral weight above a spin pseudogap of $\approx$15 meV, which is much larger than the NMR energy scale but consistent with previous neutron scattering work on underdoped $YBa_2Cu_3O_{6+x}$ (ref. 21). Second, the magnitude of the spin pseudogap implied by our data is much lower than the charge pseudogap observed in infrared spectroscopy[1]. The divergence of gap features in spin and charge channels is not unexpected in a correlated metallic state close to the Mott insulator (where the spin gap vanishes, and the charge gap is $\sim$2 eV).

We now discuss the implications of our observations for the microscopic description of the pseudogap state. Many features of the magnetic spectrum in the superconducting state are well described by models that regard the downward-dispersing branch as an excitonic mode in the spin-triplet channel below the superconducting energy gap[14,24,25]. If the downward dispersion is a manifestation of the d-wave symmetry of the gap, it is expected to disappear in the normal state, as observed. However, our observation of coherent, highly anisotropic spin excitations for $T_c < T < T^*$ requires a fresh theoretical approach. Specifically, the striking difference between the magnetic dynamics in the superconducting and pseudogap states implies that these excitations cannot simply be regarded as incoherent precursors of the resonant excitations below T_c. Rather, they seem to be a signature of a many-body state that competes with superconductivity.

The strong in-plane anisotropy of the spin dynamics in the pseudogap state offers intriguing clues to the nature of this state. The four-fold orientational symmetry of the CuO_2 planes is broken in $YBa_2Cu_3O_{6+x}$ by the CuO chains running along the b direction. However, weak-coupling calculations assuming a Fermi-liquid state above T_c in conjunction with recent angle-resolved photoelectron spectroscopy measurements[26] indicate that the hybridization between electronic states on CuO chains and CuO_2 layers is not large enough to explain the in-plane anisotropy at the low-energy end of the magnetic spectrum in the superconducting state[14]. On the basis of these model calculations[14], it is quite unlikely that band-structure effects alone can explain the much larger in-plane anisotropy and the strong temperature dependence we have observed above T_c. The low-energy spin dynamics in the pseudogap state thus seems to reflect a susceptibility of the two-dimensional electron system to a weak in-plane symmetry-breaking field (induced by the CuO chains) that is markedly larger than that of a weakly renormalized Fermi liquid. Two possibilities have been discussed recently: (1) a 'striped' state with a quasi-one-dimensional order of spins and charges that breaks rotational and translational symmetry[27,28] and (2) a 'nematic' or 'Pomeranchuk' state that breaks only the rotational symmetry[5–8]. Experimental evidence for rotational-symmetry breaking has also been gleaned from transport experiments[29].

A static striped state can be ruled out for $YBa_2Cu_3O_{6.6}$ on the basis of the two-dimensional geometry of the high-energy spin excitations (Fig. 3), and on the absence of Bragg reflections indicative of static spin and charge order. However, predictions for the spin dynamics of fluctuating stripe[17] and Pomeranchuk states[19] bear some resemblance to our data. Specifically, fluctuating stripe segments with correlation lengths of the order of a few lattice spacings can result in an approximately 'vertical', highly anisotropic dispersion surface at low energies, whereas the high-energy excitations are isotropic, as observed. However, calculations that explicitly consider the influence of superconductivity on the spin excitations of striped states[30] show only a modest effect (namely, the opening of a spin gap), in disagreement with our observations. Calculations for itinerant electron systems close to a Pomeranchuk instability[19] are also in good overall agreement with our data; however, in the superconducting state, the low-energy anisotropy of the spectral weight is significantly weaker than observed. Despite these promising first steps, an explanation of the unusual spin dynamics we have observed therefore remains an interesting challenge for theory. Its relationship to other fingerprints of the pseudogap state, such as the presence of vortex-like excitations[9] and unconventional magnetic order[10], is also not understood at present.

The full in-plane momentum resolution we have now achieved also opens a new window on the universality of the spin excitations in the cuprates. The high-energy spin excitations with four peaks along the diagonals of the CuO_2 plaquettes are indeed common

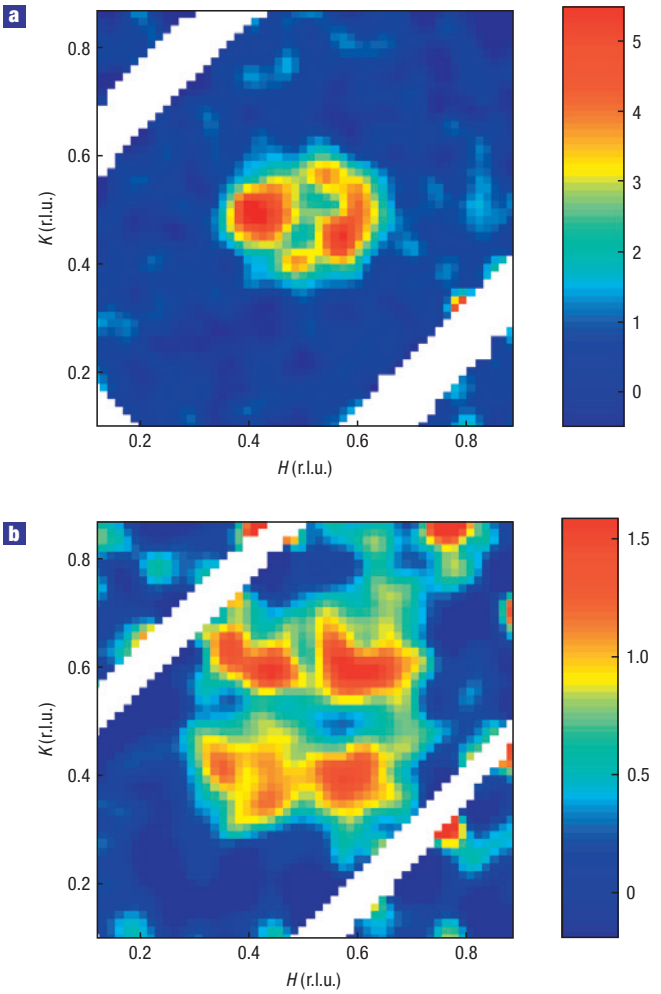

Figure 3 Colour representation of the in-plane magnetic intensity collected at the TOF spectrometer at 5 K. The incident energy was fixed to $E_i = 120$ meV and the counting time was 48 h. **a**,**b**, The intensity was integrated over the energy range $E = (30 \pm 3.5)$ meV (**a**) and over $E = (63 \pm 5)$ meV (**b**). The data represent acoustic excitations and were collected close to the maximum L component at $L = 2.1$ and 4.7, respectively (see the Methods section). A background quadratic in **Q** was subtracted and data are shown in arbitrary units.

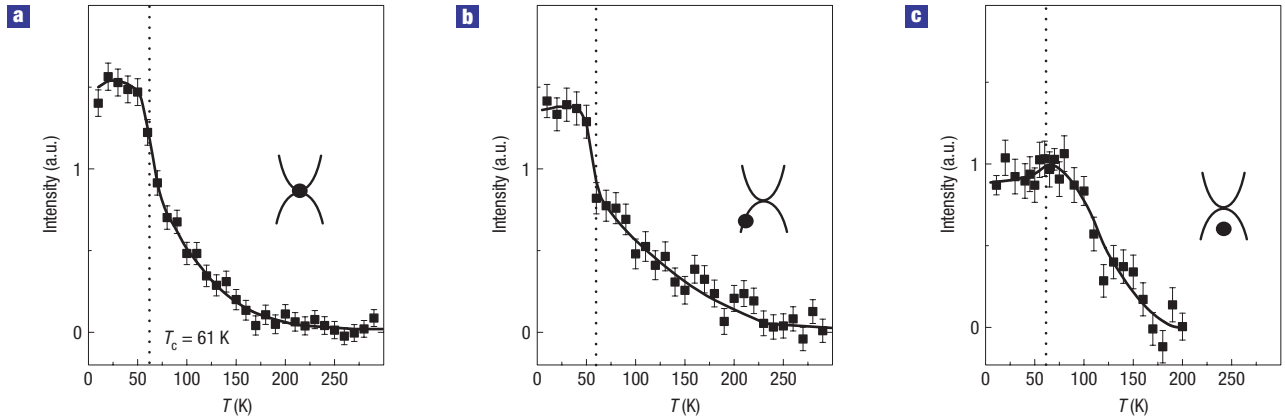

Figure 4 Temperature dependence of the peak intensity at three different positions in energy–momentum space in reference to the hour-glass dispersion in the superconducting state. a–c, The energy transfer and wavevector transfer were fixed to $E = 37$ meV and $\mathbf{Q} = (0.5, 1.5, 1.7)$ (**a**), $E = 30$ meV and $\mathbf{Q} = (1.5, 0.41, 1.7)$ (**b**) and $E = 30$ meV and $\mathbf{Q} = (0.5, 1.5, 1.7)$ (**c**). A weighted average of the background measured at two representative points was subtracted. The units in the three panels were scaled to approximately the same intensity at T_c. The error bars indicate the statistical error.

to all layered cuprate compounds thus far investigated. These excitations do not show marked changes at T_c, and their intensity distribution exhibits at most a weak in-plane anisotropy. Our data show that the geometry and spectral weight distribution at lower energies depends more strongly on materials and temperature. In particular, we have shown that the spectra in the normal and superconducting states are qualitatively different. These differences may reflect the competition between high-temperature superconductivity and other ordering phenomena such as 'nematic' or 'Pomeranchuk' states.

METHODS

The experiments were carried out on an array of 180 individually detwinned $YBa_2Cu_3O_{6.6}$ crystals with superconducting transition temperatures (midpoint) of $T_c \approx 61$ K and widths $\Delta T_c \approx 2$ K, determined for each crystal by magnetometry[13]. They were co-aligned on three Al plates with a mosaicity of $< 1.2°$. The volume of the entire array was $\sim 450\ mm^3$, and the twin-domain population ratio was 94:6.

Triple-axis measurements (Figs 1, 2 and 4) were carried out at the IN8 spectrometer at the Institut Laue Langevin (Grenoble, France) and the 2T spectrometer at the Laboratoire Léon Brillouin (Saclay, France). At both instruments, horizontally and vertically focusing crystals of pyrolytic graphite, set for the (002) reflection, were used to monochromate and analyse the neutron beam. Scans along a^* and b^* were carried out under identical instrumental resolution conditions by working in two different Brillouin zones, $(H, -1.5, -1.7)$ and $(1.5, K, 1.7)$. No collimators were used, to maximize the neutron flux, and graphite filters extinguished higher-order contamination of the neutron beam. Extensive resolution calculations confirm that the effects discussed in the main text are not resolution effects. Specifically, the spectra at 70 K exhibit only structures that are significantly broader than the resolution function, so that the observed spectrum is almost undistorted by resolution effects.

TOF measurements (Fig. 3) were carried out at the MAPS spectrometer of the ISIS spallation source, Rutherford Appleton Laboratory (Chilton, UK). The source proton current was 170 μA and the Fermi-chopper rotation frequency was set to 250 Hz.

The wavevector is quoted in units of the reciprocal lattice vectors a^*, b^* and c^* where $a = 2\pi/a^* = 3.82$ Å, $b = 3.87$ Å and $c = 11.7$ Å. We choose its out-of-plane component $L_0 = 1.7 \times (2n+1)$, n integer, to probe magnetic excitations that are odd under the exchange of two layers within a bilayer unit. As even excitations show a gap of ≈55 meV and are much less T dependent, they are presented elsewhere[25]. The incommensurability, δ, is defined as the deviation of the peak position from $\mathbf{Q}_{AF} = (0.5, 0.5)$. Even in the case where two incommensurate peaks are close together or broad (flat-top structure), δ can be obtained by fitting gaussians to the data.

Received 6 December 2006; accepted 6 August 2007; published 16 September 2007.

References

1. Timusk, T. & Statt, B. W. The pseudogap in high-temperature superconductors: An experimental survey. *Rep. Prog. Phys.* **62**, 61–122 (1999).
2. Hayden, S. M., Mook, H. A., Dai, P., Perring, T. G. & Dogan, F. The structure of the high-energy spin excitations in a high-transition-temperature superconductor. *Nature* **429**, 531–534 (2004).
3. Pailhès, S. *et al.* Resonant magnetic excitations at high energy in superconducting $YBa_2Cu_3O_{6.85}$. *Phys. Rev. Lett.* **93**, 167001 (2004).
4. Reznik, D. *et al.* Dispersion of magnetic excitations in optimally doped superconducting $YBa_2Cu_3O_{6.95}$. *Phys. Rev. Lett.* **93**, 207003 (2004).
5. Kivelson, S. A., Fradkin, E. & Emery, V. J. Electronic liquid-crystal phases of a doped Mott insulator. *Nature* **393**, 550–553 (1998).
6. Halboth, C. J. & Metzner, W. d-wave superconductivity and Pomeranchuk instability in the two-dimensional Hubbard model. *Phys. Rev. Lett.* **85**, 5162–5165 (2000).
7. Yamase, H. & Kohno, H. Possible quasi-one-dimensional Fermi-surface in $La_{2-x}Sr_xCuO_4$. *J. Phys. Soc. Jpn* **69**, 332–335 (2000).
8. Kee, H.-Y., Kim, E. H. & Chung, C.-H. Signatures of an electronic nematic phase at the isotropic-nematic phase transition. *Phys. Rev. B* **68**, 245109 (2003).
9. Wang, Y. *et al.* Dependence of upper critical field and pairing strength on doping in cuprates. *Science* **299**, 86–89 (2003).
10. Fauque, B. *et al.* Magnetic order in the pseudogap phase of high-T_c superconductors. *Phys. Rev. Lett.* **96**, 197001 (2006).
11. Tranquada, J. M. *et al.* Quantum magnetic excitations from stripes in copper oxide superconductors. *Nature* **429**, 534–538 (2004).
12. Christensen, N. B. *et al.* Dispersive excitations in the high-temperature superconductor $La_{2-x}Sr_xCuO_4$. *Phys. Rev. Lett.* **93**, 147002 (2004).
13. Hinkov, V. *et al.* Two-dimensional geometry of spin excitations in the high-transition-temperature superconductor $YBa_2Cu_3O_{6+x}$. *Nature* **430**, 650–653 (2004).
14. Schnyder, A., Manske, D., Mudry, C. & Sigrist, M. Theory for inelastic neutron scattering in orthorhombic high-T_c superconductors. *Phys. Rev. B* **73**, 224523 (2006).
15. Seibold, G. & Lorenzana, J. Magnetic fluctuations of stripes in the high temperature cuprate superconductors. *Phys. Rev. Lett.* **94**, 107006 (2005).
16. Uhrig, G. S., Schmidt, K. P. & Grüninger, M. Unifying magnons and triplons in stripe-ordered cuprate superconductors. *Phys. Rev. Lett.* **93**, 267003 (2004).
17. Vojta, M., Vojta, T. & Kaul, R. K. Spin excitations in fluctuating stripe phases of doped cuprate superconductors. *Phys. Rev. Lett.* **97**, 097001 (2006).
18. Yao, D. X., Carlson, E. W. & Campbell, D. K. Magnetic excitations of stripes and checkerboards in the cuprates. *Phys. Rev. B* **73**, 224525 (2006).
19. Yamase, H. & Metzner, W. Magnetic excitations and their anisotropy in $YBa_2Cu_3O_{6+x}$: Slave-boson mean-field analysis of the bilayer *t–J* model. *Phys. Rev. B* **73**, 214517 (2006).
20. Dai, P. *et al.* The magnetic excitation spectrum and thermodynamics of high-T_c superconductors. *Science* **284**, 1344–1347 (1999).
21. Fong, H. F. *et al.* Spin susceptibility in underdoped $YBa_2Cu_3O_{6+x}$. *Phys. Rev. B* **61**, 14773–14786 (2000).
22. Stock, C. *et al.* Dynamic stripes and resonance in the superconducting and normal phases of $YBa_2Cu_3O_{6.5}$ ortho-II. *Phys. Rev. B* **69**, 014502 (2004).
23. Bourges, P. *et al.* The spin excitation spectrum in superconducting $YBa_2Cu_3O_{6.85}$. *Science* **288**, 1234–1237 (2000).
24. Eschrig, M. The effect of collective spin-1 excitations on electronic spectra in high-T_c superconductors. *Adv. Phys.* **55**, 47–183 (2006).

25. Pailhès, S. *et al.* Doping dependence of bilayer resonant spin excitations in (Y,Ca)$Ba_2Cu_3O_{6+x}$. *Phys. Rev. Lett.* **96**, 257001 (2006).
26. Zabolotnyy, V. B. *et al.* Momentum and temperature dependence of renormalization effects in the high-temperature superconductor $YBa_2Cu_3O_{7-\delta}$. *Phys. Rev. B* **76**, 064519 (2007).
27. Tranquada, J. M., Sternlieb, B. J., Axe, J. D., Nakamura, Y. & Uchida, S. Evidence for stripe correlations of spins and holes in copper oxide superconductors. *Nature* **375**, 561–563 (1995).
28. Kivelson, S. A. *et al.* How to detect fluctuating stripes in the high-temperature superconductors. *Rev. Mod. Phys.* **75**, 1201–1241 (2003).
29. Ando, Y., Segawa, K., Komiya, S. & Lavrov, A. N. Electrical resistivity anisotropy from self-organized one dimensionality in high-temperature superconductors. *Phys. Rev. Lett.* **88**, 137005 (2002).
30. Andersen, B. M. & Hedegård, P. Spin dynamics in the stripe phase of the cuprate superconductors. *Phys. Rev. Lett.* **95**, 037002 (2005).

Acknowledgements

We thank C. Bernhard, G. Khaliullin, J. Lorenzana, D. Manske, W. Metzner, G. Seibold, M. Vojta and H. Yamase for stimulating discussions and M. Raichle and M. Bröll for support with the sample preparation. This work was supported in part by the Deutsche Forschungsgemeinschaft in the consortium FOR538.
Correspondence and requests for materials should be addressed to B.K.
Supplementary Information accompanies this paper on www.nature.com/naturephysics.

Competing financial interests

The authors declare no competing financial interests.